Since January 2020 Elsevier has created a COVID-19 resource centre with free information in English and Mandarin on the novel coronavirus COVID-19. The COVID-19 resource centre is hosted on Elsevier Connect, the company's public news and information website.

Talanta 225 (2021) 122064

Contents lists available at ScienceDirect

Talanta

journal homepage: www.elsevier.com/locate/talanta

Synthesis of polystyrene-based fluorescent quantum dots nanolabel and its performance in H5N1 virus and SARS-CoV-2 antibody sensing

Chengfei Li [a,c,d,1], Zhong Zou [a,c,d,1], Huiqin Liu [b], Yu Jin [b], Guangqiang Li [b], Chao Yuan [b,**], Zhidong Xiao [b,***], Meilin Jin [a,c,d,*]

[a] State Key Laboratory of Agricultural Microbiology, Huazhong Agricultural University, Wuhan, 430070, PR China
[b] College of Science, Huazhong Agricultural University, Wuhan, 430070, China
[c] College of Veterinary Medicine, Huazhong Agricultural University, Wuhan, 430070, PR China
[d] Key Laboratory of Development of Veterinary Diagnostic Products, Ministry of Agriculture, Wuhan, 430070, PR China

ARTICLE INFO

Keywords:
QDs nanobeads
Suspension microarray
Fluorescent lateral flow assay
SARS-CoV-2
H5N1

ABSTRACT

Quantum dots (QDs) based fluorescent nanobeads are considered as promising materials for next generation point-of-care diagnosis systems. In this study, we carried out, for the first time, the synthesis of QDs nanobeads using polystyrene (PS) nanobead as the template. QDs loading on PS nanobead surface in this method can be readily achieved by the use of polyelectrolyte, avoiding the time-consuming and uncontrollable silane reagents-involved functionalization procedure that conventional synthesis of silica-based QDs nanobeads often suffer from. Notably, the application of QDs nanobeads in suspension microarray for H5N1 virus detection leads to a sensitivity lower than 25 PFU/mL. In addition, QDs nanobead was also incorporated into lateral flow assay for SARS-CoV-2 antibody detection, leading to more than one order of magnitude detection sensitivity as compared to that of commercial one based on colloid gold.

1. Introduction

Quantum Dots (QDs), due to their unique optical-electronic properties compared to traditional labeling reagents (organic-and protein-based fluorophores), has been attracting wide interest in bioimaging and biosensing, and a significant progress has been made thanks to the sophisticated surface coating technology developed especially for CdSe@ZnS core-shell QDs [1–12]. However, to the best of our knowledge, most of previous reported QDs-based fluorescence methods for bioassay always suffer from low sensitivity compared to that of clinic ones, such as chemical luminescence immunoassay (CLIA) [13], digital enzyme-linked immunosorbent assay (digital ELISA) [7], and time-resolved fluorescence immunoassay (TRFIA) [14], among which the sensitivity for protein detection could reach subfemtomolar concentration. This partially could be ascribed to the difficulty on the synthesis of coating reagents that can render QDs biocompatible and fluorescence-stable over a long period of time [15–17]. In addition, the increased hydrodynamic size and decreased fluorescence yield brought by QDs phase transfer further make their initial superiority less obvious, as compared to their counterparts. Therefore, how to overcome these defects plays a vital role in development of QDs-based bioassay technology with ultrahigh sensitivity, which could contribute to the clinic application of QDs technology in bioassay. Gao et al. recently reported work developed a QDs based fluorescence bioassay capable of dramatically improving the sensitivity of virtually all common biodetection techniques including ELISA, lateral flow strips and suspension microarray by approximately three orders of magnitude [5]. The mechanism behind involved the densely adsorption of individual PEG–NH_2–capped QDs on the surface of HRP-catalysed polydopamine deposited on secondary antibody and nearby proteins, leading to huge fluorescence signal amplification. Nonetheless, the use of oxidant H_2O_2 at high concentration and the fresh preparation requirement of deposition solution are the innegligible drawbacks in practical application.

QDs encapsulation in silica nanobeads is an alternative widely adopted as signal amplification materials for the development of bioassay with improved sensitivity [18–24]. Typically, the synthesis

* Corresponding author. State Key Laboratory of Agricultural Microbiology, Huazhong Agricultural University, Wuhan, 430070, PR China.
** Corresponding author.
*** Corresponding author.
E-mail addresses: yuanchao@mail.hzau.edu.cn (C. Yuan), zdxiao@mail.hzau.edu.cn (Z. Xiao), jinmeilin@mail.hzau.edu.cn (M. Jin).
[1] These authors contributed equally to this work.

https://doi.org/10.1016/j.talanta.2020.122064
Received 5 October 2020; Received in revised form 7 December 2020; Accepted 23 December 2020
Available online 2 January 2021

fluorescence nanobeads involves the immobilization of QDs on the surface of colloidal silica realized by amino-group mediated electrostatic interaction or thiol-group driven coordination, followed by silica shell coating for the purpose of fluorescence stabilization and functionalization. To data, nonporous [18–22] and dendritic silica [23,24] are the chief templates for QDs assembly, among which dendritic silica featured with ultralarge pore channels and highly accessible inner surface exhibits obvious superiority for QDs loading and application in sensitive bioassay as compared with its counterparts. In addition, polystyrene (PS) bead, due to its sophisticated synthesis technique, is the core material commonly served as the suspension carrier for the immobilization of capture antibody in the above mentioned techniques [7]. Most importantly, as compared with silica, Coefficient of Variance value of monodisperse PS beads could reach 3% with good reproducibility, much less than that of commercial silica particles (typically 10–15%), and the abundance of carboxyl group on their surface could be precisely controlled by adjusting the ratios of reactants. However, to the best of our knowledge, PS beads-based template for development of QDs nanobeads as labeling material has not been reported. Herein, highly fluorescent 200 nm QDs nanobead was fabricated using commercially-available PS beads as absorbent host and CdSe@ZnS QDs nanoparticles, followed by a silica shell coating for protection and further biosensing. The fluorescence properties of this nanobead was characterized and compared with commercially available fluoro-max fluorescent beads with europium chelate, and finally its performance on sensitive detection of H5N1 virus and SARS-CoV-2 antibody as fluorescence reporter in flow cytometry and lateral flow strips was systematically evaluated, respectively.

2. Experimental section

2.1. Reagents and materials

Poly(diallydimethyl) ammonium chloride (PDAMAC; MW 15000), tetraethylorthosilicate (TEOS), 3-Aminopropyltriethoxysilane (APTS), 2-Morpholinoethanesulfonic acid (MES), mouse IgG, rabbit anti-mouse IgG, fetal bovine serum (FBS), 1-Ethyl-3-(3-(dimethylamino)propyl) carbodiimide (EDC), N-hydroxysuccinimide (NHS), 3-mercaptopropionic acid (MPA), poly(vinylpyrrolidone) (PVP; MW 55000) and succinic anhydride were purchased from Sigma-Aldrich (Shanghai, China). All DNA samples used in this work were synthesized by Sangon Biotechnology Co., Ltd (Shanghai, China). CdSe@ZnS quantum dots were provided from Xingshuo Biotechnology Co., Ltd (Suzhou, China). Fluoro-max fluorescent beads with europium chelate was provided from Thermo Fisher Scientific Inc. COOH-coated polystyrene (PS) microbeads (0.2 and 4 μm) were obtained from Huge Biotechnology Co., Ltd (China). SARS-CoV-2 (2019-nCoV) Spike RBD-His Recombinant Protein were obtained from Sino Biological (Beijing). Influenza A virus H5N1 HA (Hemagglutinin) antibody were purchased from Gene Tex. The H5N1 virus strain, isolated from chicken and stored by our lab, was cultured in SPF chicken embryo and stored at −80 °C. The viruses were amplified using 10-day-old embryonic chicken eggs and then titrated by determining log10 TCID50/ml values on MDCK cells. SARS-CoV-2 positive and negative serum were kindly provided by Renmin Hospital of Wuhan University. All experiments with the H5N1 virus were performed in a Biosafety Level 3 Laboratory (BSL-3). This study was carried out in accordance with the recommendations of BSL-3 laboratory at Huazhong Agricultural University (HZAU). All procedures were approved by the Intuitional Biosafety Committee of HZAU. Ultrapure water (18.2 MΩ) was used from a Millipore water purification system.

2.2. Synthesis of magnetic microbeads and surface functionalization

Citrate-capped Fe_3O_4 nanoparticles with the diameter of ~10 nm were prepared according to our previously reported method [25]. For synthesizing the magnetic microbeads, 100 mL of the COOH-capped polystyrene microbeads (5 mg/mL) were initially incubated with 100 mL of NaCl solution containing 2 mL of polyelectrolyte PDAMAC for 3 h under rotation. After washing with water for three times by centrifugation, the microbeads were resuspended in 100 mL of water and mixed 40 mL of Fe_3O_4 nanoparticle solution using ultrasonication, followed by magnetic separation by a magnet to purify the obtained Fe_3O_4 nanoparticles-immobilized magnetic microbeads from the mixture. The obtained magnetic microbeads were then incubated with PVP solution (1 mM) overnight. For silica coating, PVP-coated magnetic microbeads were suspended in a mixture of isopropanol (200 mL) and water (40 mL) containing 4 mL of ammonia, and 0.5 mL of TEOS were equally added into the mixture by 5 times with 3-h interval. APTS (0.1 mL) were added into the mixture at last for another 4 h reaction to obtain the amino-functionalized silica-coated magnetic microbeads. For further biomolecule conjugation, amino group on the surface of microbeads were transferred into carboxyl group by incubating the microbeads in 100 mL of acetone solution containing 50 mg succinic anhydride for 6 h to obtained carboxyl group-capped magnetic microbeads. The obtained carboxyl-capped magnetic microbeads were washed with water for three times and then suspended in 10 mL MES buffer (pH = 4.8) containing 10 mg of EDC and 6 mg of NHS for 15 min under rotation. For antibody conjugation, the activated carboxyl-capped magnetic microbeads were then washed with 1 × PBS for three times and suspended in 1 mL of PBS buffer containing anti-H5N1 antibody (1 mg/mL). After rotation for 6 h, the microbeads were washed with 1 × PBS for three times and stored in 100 μL of 1 × PBS buffer containing 0.5% BSA for further use.

2.3. Synthesis of QDs nanobeads and functionalization

Commercial TOPO-capped CdSe@ZnS QDs were first transferred into water by 3-mercaptopropionic acid according to a reported method [26]. For QDs nanobeads preparation, COOH-capped 200 nm polystyrene beads (20 mg) were treated with NaOH solution (4 mL, 1 mM) for 5 min, followed by incubating with 10 mL of NaCl solution containing 0.2 mL of polyelectrolyte PDAMAC for 3 h with rotation. After washing with water for three times by centrifugation, the beads were resuspended in 20 mL of water and mixed with 10 mL of CdSe@ZnS QDs solution using ultrasonication, followed by centrifugation to purify the obtained QDs-immobilized fluorescent beads from the mixture. The obtained fluorescent beads were then incubated with PVP solution (1 mM) overnight. For silica coating, PVP-coated fluorescent beads were suspended in a mixture of isopropanol (20 mL) and water (4 mL) containing 1 mL of ammonia, and 0.1 mL of TEOS were equally added into the mixture by 5 times with 3-h interval. APTS (0.05 mL) were added into the mixture at last for another 4 h reaction to obtain the amino-functionalized silica-coated fluorescent beads. Amino group on the surface of beads were then transferred into carboxyl group by incubating them in 10 mL acetone solution containing 10 mg succinic anhydride for 6 h. The obtained carboxyl-capped fluorescent nanobeads were washed with water for three times and then suspended in 10 mL MES buffer (pH = 4.8) containing 10 mg of EDC and 6 mg of NHS for 15 min under rotation. For anti-H5N1 antibody conjugation, the activated carboxyl-capped fluorescent nanobeads were washed with 1 × PBS for three times and suspended in 1 mL of PBS buffer containing anti-H5N1 antibody (1 mg/mL). After rotation for 6 h, the nanobeads were washed with 1 × PBS for three times and stored in 100 μL of 1 × PBS buffer containing 0.5% BSA for further use.

2.4. Suspension microarray with QDs nanobeads for H5N1 virus detection

Avian influenza virus (AIV) H5N1 A/duck/Hubei/xn/2007 (H5N1; designated as XN/07) (Genbank accession number of HA: AHI43271.1) was propagated in the allantoic cavities of 9-day old specific pathogen-free (SPF) embryonated chicken eggs and stored at −80 °C. PBS

containing BSA (0.5%) was used as incubation and blocking buffer throughout the experiment, and all washing steps were done by magnetic separation with an external magnet at room temperature for 2 min. For H5N1 virus detection, 5 μL of antibody-coated microbeads (1×10^8 beads/mL) were added into 45 μL of virus solution with varied concentrations. After incubation the mixture under gentle rotation for 1.5 h, the microbeads were washed three times with PBS (0.5% BSA) and resuspended in 50 μL PBS (0.5% BSA). Then 5 μL antibody-coated QDs nanobeads (1×10^{12} beads/mL) were added into the microbeads solution for another 1.5 h incubation under gentle rotation. After washing three times, the microbeads were then analyzed by flow cytometry equipped with a 488 nm excitation wavelength. For each sample, 10000 microbeads were counted for analysis.

2.5. Lateral flow assay for SARS-CoV-2 antibody detection using QDs nanobead

The method for immobilization of RBD protein and mouse IgG on the surface of QDs nanobead is similar to that of the preparation of H5N1 antibody-coated QDs nanobead. Briefly, 20 μL of QDs nanobead (10 mg/mL) were suspended in 1 mL MES buffer (pH = 4.8) containing 20 mg of EDC and 12 mg of NHS. After rotating for 30 min, the activated QDs nanobead were washed with PBS for three times and suspended in 1 ml PBS. Then, RBD protein (2 μg) or mouse IgG (1 μg) were added the solution for 3 h incubation, followed by addition of 10 μL of 10% BSA to block the activated carboxyl groups for 1 h. After washing with PBS for three times. The obtained RBD protein- and mouse IgG-coated QDs nanobead were stored in 1 mL of PBS (0.5% BSA) and stored at 4 °C for further use, respectively.

The test strip is consisted of plastic backing, sample pad, conjugation pad, absorbent pad, NC membranes. A dispenser system was used to load a set volume of RBD protein- and mouse IgG-coated QDs nanobead onto the conjugation pad and then dried at 37 °C for overnight. To prepare the NC membrane, RBD protein (0.8 mg/mL) and rabbit anti mouse IgG (1.0 mg/mL) were dispensed onto the test line (T-line) and control line (C-line) on NC membranes and dried at 37 °C for 6 h, respectively. All of that was dispensed at the rate of 1.0 μL/cm using dispense platform. And then test strip were cut to individual 4 mm wide strips using a programmable cutting machine. Finally, the strips were installed in a plastic case for the following assay.

For SARS-CoV-2 antibody detection, a series of 75 μL of serum with different dilution ratios were added to the sample well. The liquid migrated towards the absorption pad by capillary action. After 15 min, the preliminary results were observed with naked eye by portable UV lamp. To evaluate the sensitivity of our test strip, an intelligent fluorescent strip reader was used to read out the result.

2.6. Characterization

Surface charges of polystyrene beads were determined by a Zetasizer Nano ZS (Malvern Instruments, UK). Fluorescence imaging of individual microbeads based nanoMBs were collected by confocal laser scanning microscope (Leica TCS-SP5II, Germany). SEM images of magnetic microbeads were obtained by scanning electron microscope (SEM, FEI Quanta 200F), TEM images of magnetic microbeads and QDs nanobeads were obtained by transmission electron microscope (TEM, Philips CM 300). Fluorescence measurements were carried out by a flow cytometry equipped with a 488 nm laser (CytoFLEX S from Beckman Coulter). A XYZ3200 series system and a programmable strip cutter were obtained from Bio-Dot scientific Equipment (Burton, MI, USA). A fluorescent strip test reader (AFS-1000) was purchased from Guangzhou lanbo Biotechnology.

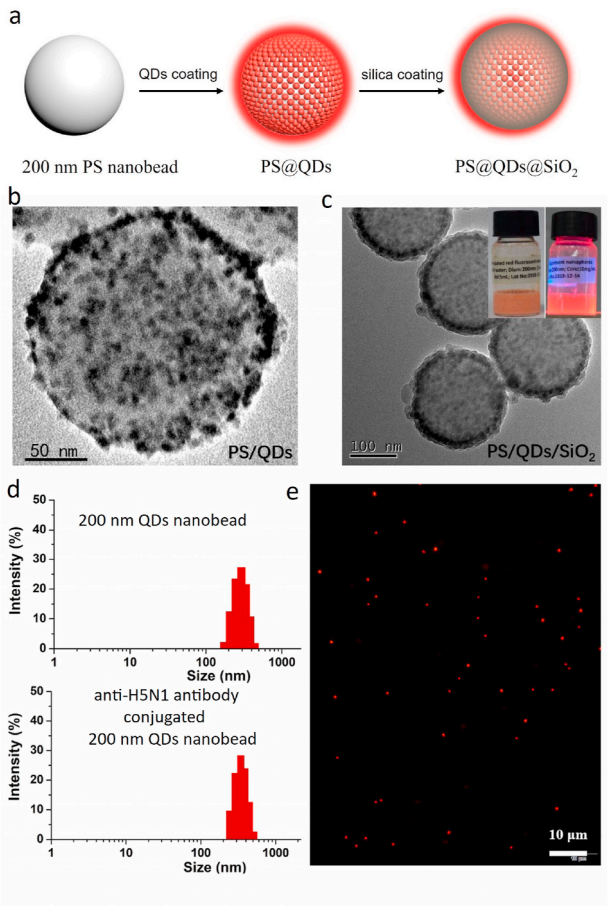

Fig. 1. a) Synthesis route of 200 nm fluorescence QDs nanobeads (PS@QDs@SiO_2). b) TEM image of PS@QDs. c) TEM image of PS@QDs@SiO_2. Insets: photo images of aqueous solution under natural light and UV lamp, respectively. d) Particle size distribution of 200 nm PS@QDs@SiO_2 before and after antibody conjugation. e) Fluorescence image of the obtained PS@QDs@SiO_2 under the excitation wavelength of 365 nm.

3. Results and discussion

3.1. Synthesis and characterization of QDs nanobeads

CdSe@ZnS QDs nanobeads were prepared using layer-by-layer method using polystyrene (PS) nanobeads with the diameter of 200 nm as the template, as shown in Fig. 1a. Briefly, polyelectrolyte PDAMAC was used to render commercial COOH-capped PS nanobeads surface positively-charged, followed by incubation with excess of mercaptopropionic acid-capped QDs under ultrasonication to obtain a homogenous solution for fluorescence attachment. Due to the electrostatic interaction between nanobeads and QDs, the surfaces of PS nanobeads were densely decorated with these fluorescent nanoparticles, which could be clearly confirmed by TEM image in Fig. 1b. The color of the QDs nanobeads solution under natural and UV light in the inset photos in Fig. 1c could also confirm the successful decoration of QDs on the surface of PS nanobeads. The obtained fluorescent nanobeads (PS@QDs) were then coated with silica shell for fluorescence protection and further bio-functionalization. As shown in Fig. 1c, the prepared PS@QDs were uniformly coated with a thin SiO_2 shell with narrow size distribution, which could be further confirmed by size distribution data (top in Fig. 1d). In addition, after antibody conjugation, the QDs nanobead was instantaneously redispersed in PBS without obvious size change (bottom in Fig. 1d). The fluorescence property of the obtained QDs nanobead was also investigated. As shown in Fig. 1e, single QDs nanobead could be clearly observed with bright fluorescence under

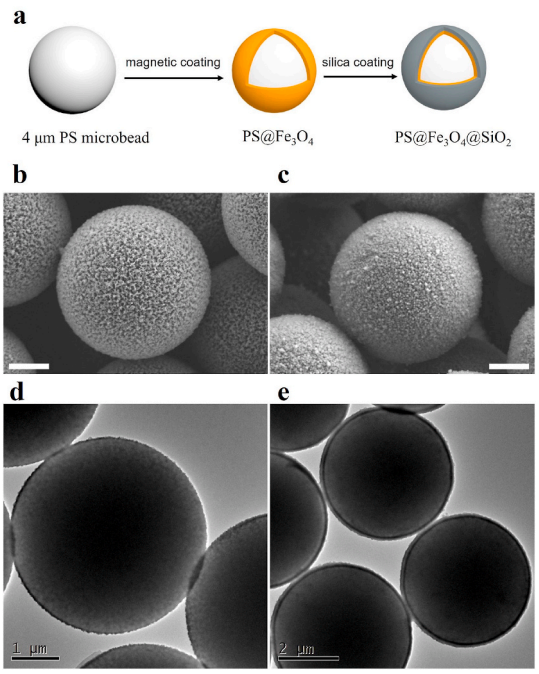

Fig. 2. a) Synthesis route of 4 μm magnetic microbeads. b) and d) represent the SEM and TEM images of Fe_3O_4 nanoparticles densely-decorated polystyrene microbeads (PS@Fe_3O_4), respectively. c) and e) represent the SEM and TEM images of the obtained magnetic microbeads with a silica shell (PS@Fe_3O_4@SiO_2), respectively. Both of the scale bars in b) and c) are 1 μm.

fluorescence microscopy. In addition, the fluorescence brightness of the prepared QDs nanobead is comparable to that of commercial fluoro-max fluorescent beads with europium chelate at the same diameter (Fig. S1 in Supporting Information).

3.2. Synthesis of magnetic microbeads for flow cytometry assay

Note that, like micro-size polystyrene beads, QDs nanobead with the diameter of 200 nm would also be distinguished by flow cytometry due to its big size. In this work, in order to eliminate the interference brought by free QDs nanobead that not specifically adsorbed on PS beads, magnetic microbead, instead of traditional PS bead, was used as the carrier for immunoassay in flow cytometry. Herein, magnetic microbeads with the diameter of 4 μm were synthesized according to our previously reported method [25], as shown in Fig. 2a. Typically, positively-charged PS microbeads were mixed with excess of negatively-charged Fe_3O_4 nanoparticles under ultrasonication to obtain a homogenous solution. Due to the electrostatic interaction between microbeads and Fe_3O_4 nanoparticles, the surfaces of PS microbeads were densely decorated with these magnetic nanoparticles, realizing the easy purification of magnetic microbeads from the mixture solution simply by an external magnet. After washing three time with water, the magnetic microbeads were coated with a shell of silica by TEOS and surface amination by APTS. The amino group were then reacted with succinic anhydride in acetone to functionalize the surface of magnetic microbeads with carboxyl group. Fig. 1b–d clearly shows the decoration of magnetic nanoparticles on the surface of microbeads, and a shell of silica was confirmed by the TEM image in Fig. 2e. In addition, due to the dense decoration of magnetic nanoparticles on their surface, the magnetic microbeads suspended in solution could be collected by an external magnet in 1 min and resuspended in solution simply by a pipette, which means the drawbacks including beads aggregation, decrease of biomolecule activity and poor reproducibility of the results caused by traditional tedious separation and suspension steps could be addressed simply by magnetic separation.

3.3. Construction and validation of flow cytometry-based virus sensing

Fig. 3a shows the detection procedure of H5N1 virus based on flow cytometry. Typically, anti-H5N1 antibody, as the virus probe, was immobilized both on the surface of magnetic beads and QDs nanobeads by EDC/NHS method. In the absence of H5N1 virus, QDs nanobeads would not specifically adsorbed onto the surface of magnetic beads because of the weak interaction between those two kinds of beads, resulting in the maintaining of non-fluorescence property of the magnetic beads. However, in the presence of target virus, due to the immune reaction between antibody and protein on the surface of H5N1 virus, QDs nanobeads would be adsorbed onto the surface of magnetic beads to render the magnetic beads fluorescent, which could be identified by flow cytometry. Fig. 3b is the SEM image of the magnetic bead after sequential incubation with target virus and QDs nanobeads, which clearly shows the presence of QDs nanobeads adsorbed on the surface of magnetic beads. Fig. 3c further displays the fluorescence image of the QDs nanobeads adsorbed magnetic beads, validating the feasibility of the method proposed. Interesting, it is found in this work that the concentration of virus was highly correlated with the percentage of fluorescence-positive magnetic beads. Note that the control group is conducted exactly the same to the experimental one except the presence of H5N1 virus in detection solution. As shown in Fig. 3d–k, with the increase of virus concentration from 25 to 250000 PFU/mL, the percentage of fluorescence magnetic beads gradually increased and finally reached 98.8%. Moreover, even at the virus concentration of 25 PFU/mL, the percentage of fluorescence magnetic beads dramatically increased to near 40%, as compared to the control group (12%).

For practical application, selectivity of the proposed method to other subtypes of avian influenza was also investigated. As shown in Figure 3n, due to the specificity of anti-H5N1 antibody to H5N1 virus, the response of this method to other virus including H1, H7, H9, NDV and IBDV was very weak even at the concentration of 10000 PFU/mL, demonstrating the discriminating ability of this method for H5N1 detection with high selectivity. To evaluate the performance of the proposed method to detect H5N1 virus in real sample, saliva from 9 H5N1 virus positive chicken were sampled and dissolved in PBS prior to assay. It should be noted that the presence of H5N1 virus in all the 9 chicken was verified by PCR experiment. As shown in Figure 3m, the percentages of positive beads obtained from all the 9 samples exceed the cutoff value of 12% with two obvious ones (sample 3# and 9#), indicating the presence of H5N1 virus in all the sample tested and the accuracy of our method for H5N1 virus diagnosis in practical application. The comparison of different methods for AIV H5N1detection is shown in Table 1. Compared to most existing detection methods, our quantum dots nanolabel based detection system has lower limit of detection and wider dynamic range.

3.4. Lateral flow assay for SARS-CoV-2 antibody detection

The outbreak of SARS-CoV-2 virus has killed more than 500000 people across the world, and developing highly accurate detection method for antibodies against SARS-CoV-2 is crucial to combating the pandemic [32]. Lateral flow assay, as an idea simple and low-cost bioassay technology for point-of-care test, has been widely used in our daily life for qualitative detection. Herein, QDs nanobead, instead of traditional colloid gold, was used to construct a fluorescence-based lateral flow strips for SARS-CoV-2 antibody detection, in which RBD protein and rabbit anti mouse IgG were pre-immobilized on the test and control line, respectively, and a mixture of RBD protein-coated QDs nanobeads and mouse IgG-coated QDs nanobeads were dropped and dried on the conjugated pad. The detection mechanism was shown in Fig. 4, which clearly shows that QDs nanobeads would be captured at the test line only in the presence of target antibody existed in testing sample, leading to fluorescence appearance at the display area. Several experimental parameters including RBD protein concentration for

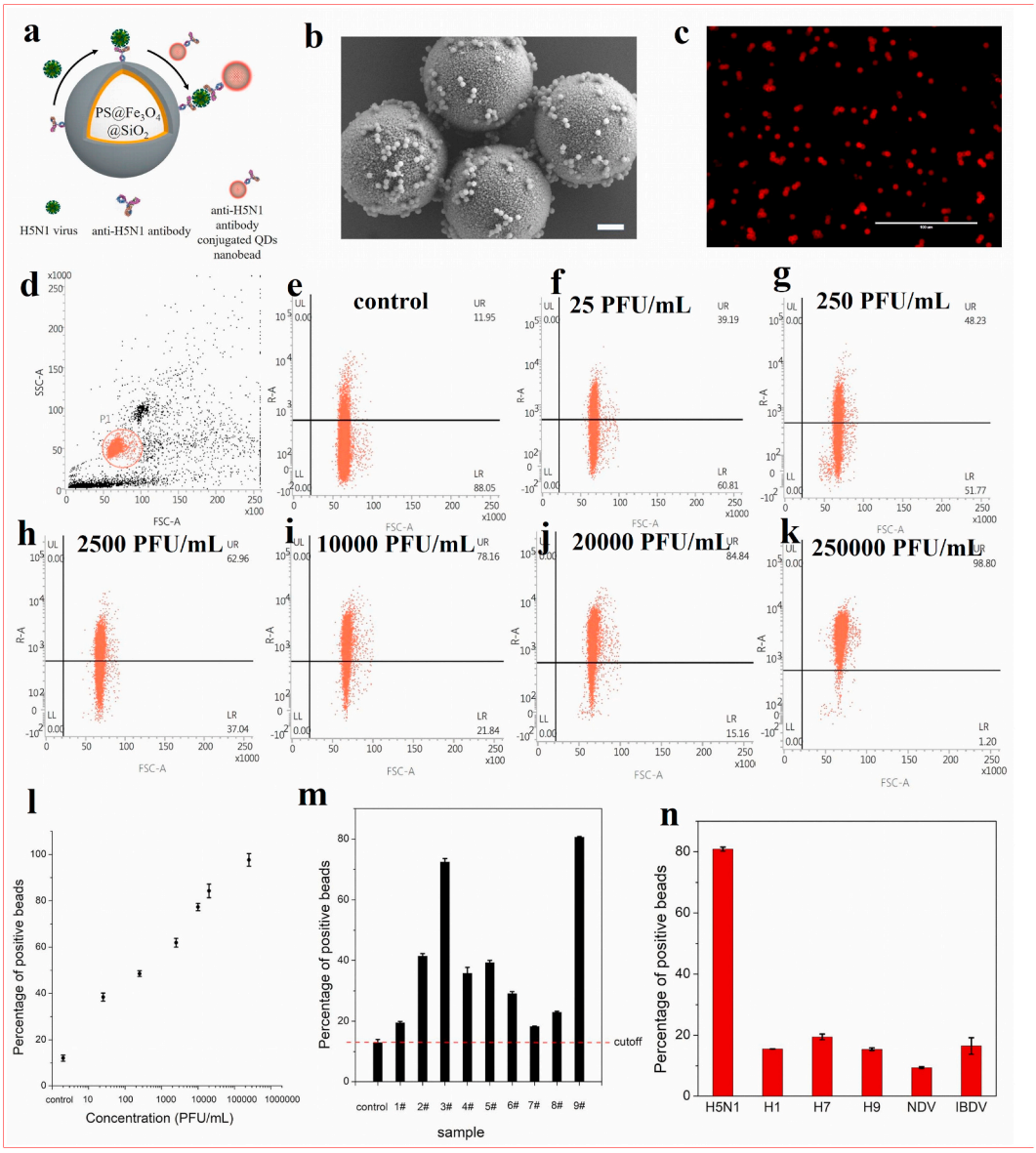

Fig. 3. a) Schematic representation of H5N1 virus detection based on 4 μm magnetic microbead and 200 nm fluorescent QDs microbead. b-c) SEM and fluorescence images of the QDs nanobead adsorbed magnetic beads, scale bar in b and c are 1 μm and 100 μm, respectively. d-k) flow cytometry data of the proposed assay. l) Plot of percentage of positive bead quantification data for H5N1 virus determination. Error bars represent the SD (n = 3). m) Performance of the proposed method for the detection of H5N1 virus from 9 positive chicken samples. All the saliva dissolved in 400 μL of PBS prior to incubation with magnetic bead. Error bars represent the SD (n = 3). n) Response of the proposed method to other subtypes of avian influenza. Error bars represent the SD (n = 3).

Table 1
Methods comparison for AIV H5N1detection.

Detection method	target	LOD	dynamic range	reference
ECL	HA	2.7×10^2 PFU/mL	2.7×10^2-2.7×10^3 PFU/mL	[27]
QCM	H5N1 HA	0.0128 HAU	0.128–12.8 HAU	[28]
SPR	H5N1 AIV	0.128HAU	0.128–1.28 HAU	[29]
Fluorescence microscope	H5N1 AIV	10^3 TCID50/mL	10^3-10^4 TCID50/mL	[30]
DMF	H5NI HA	74 pg/mL	–	[31]
Quantum dots nanolabel based detection system	H5N1 AIV	25 PFU/mL	–	present study

Notes: HA is AIV surface glycoprotein HA (Hemagglutinin).

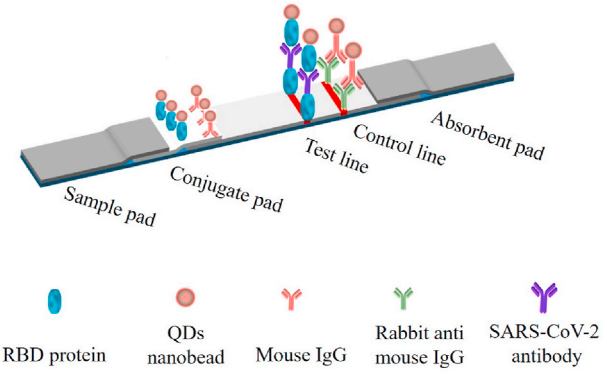

Fig. 4. Schematic illustration of lateral flow assay for SARS-CoV-2 antibody detection using QDs nanobead as the fluorescence reporter.

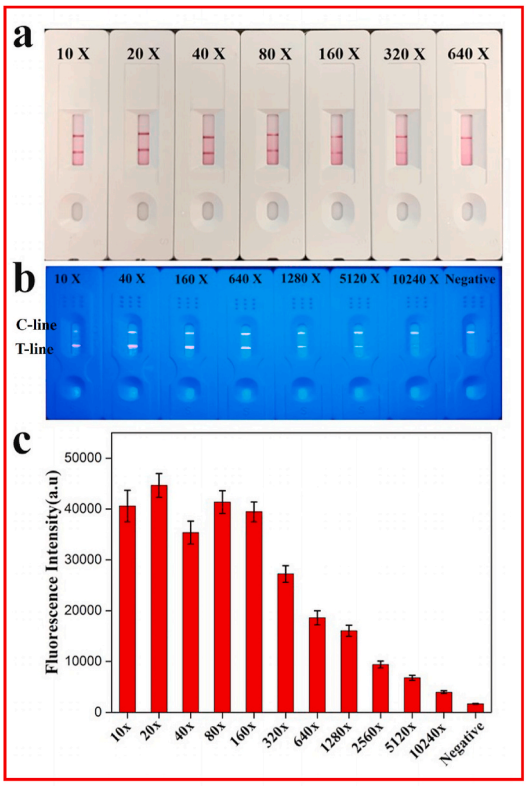

Fig. 5. Comparison of traditional colloid gold (a) and QDs nanobead (b) based lateral flow strips (LFS) for SARS-CoV-2 detection. (c) Fluorescence intensities on the test line obtained from QDs nanobead-based lateral flow assay for a series of diluted sample. Error bars represent standard deviation (n = 3). (For interpretation of the references to color in this figure legend, the reader is referred to the Web version of this article.)

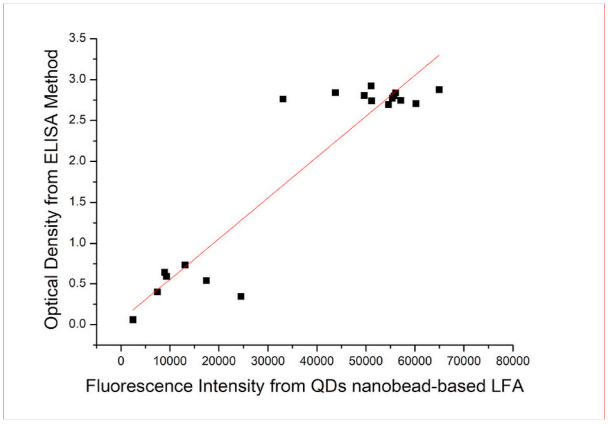

Fig. 6. Correlation analysis between traditional ELISA method and QDs nanobead based lateral flow assay (LFA) for SARS-CoV-2 antibody detection in 18 serum samples. All the serum sample tested were 1:10 diluted by PBS prior to detection.

printing, QDs nanobead concentration and fluorescence response time has been optimized (Fig. S3 in Supporting Information) for the best performance of QDs nanobead-based fluorescence method. Fig. 5a and b shows the comparison of traditional colloid gold and QDs nanobeads based lateral flow strips using the same SARS-CoV-2-positive sample with different dilution rate. For conventional method, there was no signal for the sample with 320-fold dilution, while a moderate signal still can be observed by naked-eye at the dilution factor of 10240 for QDs-nanobeads based fluorescence assay. Another advantage of fluorescence-based lateral flow strips is its capability for quantification by a commercialized fluorescence scanner. Fig. 5c shows that fluorescence intensity obtained from 10240-fold diluted sample is still much stronger than that of negative one, demonstrating improved sensitivity with more than one order of magnitude at least as compared to that of conventional one.

To further evaluate the accuracy of this method for clinical application, 18 clinic serum samples were assayed with standard ELISA or QDs nanobead-based lateral flow assay. It is found that all the samples were SARS-CoV-2 positive from ELISA test result, and that those samples (1#-12#) with high optical density obtained also gave out strong fluorescence signal by our QDs nanobead-based method (Fig. 6 and S4 in Supporting Information). Furthermore, the fluorescence intensities from samples (13#-18#) with low optical density were also weak as compared to that from other serum tested, demonstrating the accuracy of our QDs nanobead based lateral flow assay.

4. Conclusion

In summary, fluorescent QDs nanobead was synthesized for the first-time using PS nanobead as the template. Compared to the silica-based template method involving uncontrollable hydrolysis of silane reagents on silica surface for QDs loading, QDs immobilization on the surface of PS nanobead could be readily achieved by polyelectrolyte-mediated surface modification, and the fluorescence brightness of the obtained QDs nanobead is comparable to that of commercial fluoro-max fluorescent beads with europium chelate at the same diameter. Moreover, magnetic-responsive microbead was synthesized for the fabrication of suspension microarray using QDs nanobead as the fluorescence label, and as low as 25 PFU/mL sensitivity for H5N1 virus detection was achieved. The obtained QDs nanobead was also incorporated into lateral flow strip as the signal tag for the detection of SARS-CoV-2 antibody with more than one order of magnitude sensitivity as compared to commercially-available colloid gold strips, demonstrating its potential in practical application.

Credit author statement

Chengfei Li: Conceptualization, Methodology, Formal analysis, Writing – original draft. Zhong Zou: Formal analysis, Methodology, Writing – original draft, Investigation. Huiqin Liu: Investigation, Validation. Yu Jin: Methodology, Validation. Guangqiang Li: Formal analysis. Chao Yuan: Funding acquisition, Writing – review & editing. Zhidong Xiao: Writing – review & editing, Funding acquisition. Meilin Jin: Supervision, Project administration, Funding acquisition, Writing – review & editing.

Declaration of competing interest

The authors declare that they have no known competing financial interests or personal relationships that could have appeared to influence the work reported in this paper.

Acknowledgement

This work was supported by the funds of Hubei Provincial Special Emergency (2020FCA046), the National Natural Science Foundation of China (21705054), the fundamental Research Funds for Central Universities (2662019PY024), and the open funds of the State Key Laboratory of Agricultural Microbiology (AMLKF201908).

Appendix A. Supplementary data

Supplementary data to this article can be found online at https://doi.org/10.1016/j.talanta.2020.122064.

References

[1] M. Bruchez, M. Moronne, P. Gin, S. Weiss, A.P. Alivisatos, Semiconductor nanocrystals as fluorescent biological labels, Science 281 (5385) (1998) 2013–2016.

[2] W.C.W. Chan, S.M. Nie, Quantum dot bioconjugates for ultrasensitive nonisotopic detection, Science 281 (5385) (1998) 2016–2018.

[3] L. Cohen, N. Cui, Y. Cai, P.M. Garden, X. Li, D.A. Weitz, D.R. Walt, Single molecule protein detection with attomolar sensitivity using droplet digital enzyme-linked immunosorbent assay, ACS Nano 14 (8) (2020) 9491–9501.

[4] L. Cohen, D.R. Walt, Highly sensitive and multiplexed protein measurements, Chem. Rev. 119 (1) (2018) 293–321.

[5] J. Li, M.A. Baird, M.A. Davis, W. Tai, L.S. Zweifel, K.M. Adams Waldorf, M. Gale Jr., L. Rajagopal, R.H. Pierce, X. Gao, Dramatic enhancement of the detection limits of bioassays via ultrafast deposition of polydopamine, Nat. Biomed. Eng. 1 (6) (2017) 1–12.

[6] H. Mattoussi, J.M. Mauro, E.R. Goldman, G.P. Anderson, V.C. Sundar, F.V. Mikulec, M.G. Bawendi, Self-assembly of CdSe-ZnS quantum dot bioconjugates using an engineered recombinant protein, J. Am. Chem. Soc. 122 (49) (2000) 12142–12150.

[7] D.M. Rissin, C.W. Kan, T.G. Campbell, S.C. Howes, D.R. Fournier, L. Song, T. Piech, P.P. Patel, L. Chang, A.J. Rivnak, E.P. Ferrell, J.D. Randall, G.K. Provuncher, D. R. Walt, D.C. Duffy, Single-molecule enzyme-linked immunosorbent assay detects serum proteins at subfemtomolar concentrations, Nat. Biotechnol. 28 (6) (2010) 595–599.

[8] C.Y. Zhang, H.C. Yeh, M.T. Kuroki, T.H. Wang, Single-quantum-dot-based DNA nanosensor, Nat. Mater. 4 (11) (2005) 826–831.

[9] W. Zhou, Y. Han, B.J. Beliveau, X. Gao, Combining qdot nanotechnology and DNA nanotechnology for sensitive single-cell imaging, Adv. Mater. 32 (30) (2020) 1–8.

[10] P. Zrazhevskiy, X. Gao, Quantum dot imaging platform for single-cell molecular profiling, Nat. Commun. 4 (2013) 1619.

[11] P. Zrazhevskiy, M. Sena, X. Gao, Designing multifunctional quantum dots for bioimaging, detection, and drug delivery, Chem. Soc. Rev. 39 (11) (2010) 4326–4354.

[12] P. Zrazhevskiy, L.D. True, X. Gao, Multicolor multicycle molecular profiling with quantum dots for single-cell analysis, Nat. Protoc. 8 (10) (2013) 1852–1869.

[13] A. Padoan, C. Cosma, L. Sciacovelli, D. Faggian, M. Plebani, Analytical performances of a chemiluminescence immunoassay for SARS-CoV-2 IgM/IgG and antibody kinetics, Clin. Chem. Lab. Med. 58 (7) (2020) 1081–1088.

[14] Y. Zhang, X. Yang, J. Qian, X. Gu, J. Zhang, J. Liu, Z. Hu, Simultaneous detection of Mycoplasma pneumoniae IgG and IgM using dual-label time resolved fluoroimmunoassay, Anal. Biochem. 548 (2018) 1–6.

[15] J.M. Klostranec, W.C.W. Chan, Quantum dots in biological and biomedical Research: recent progress and present challenges, Adv. Mater. 18 (15) (2006) 1953–1964.

[16] I.L. Medintz, H.T. Uyeda, E.R. Goldman, H. Mattoussi, Quantum dot bioconjugates for imaging, labelling and sensing, Nat. Mater. 4 (6) (2005) 435–446.

[17] A.M. Smith, H. Duan, A.M. Mohs, S. Nie, Bioconjugated quantum dots for in vivo molecular and cellular imaging, Adv. Drug Deliv. Rev. 60 (11) (2008) 1226–1340.

[18] M. Cho, K. Lim, K. Woo, Facile synthesis and optical properties of colloidal silica microspheres encapsulating a quantum dot layer, Chem Commun (Camb) 46 (30) (2010) 5584–5586.

[19] J. Li, Y. Lv, N. Li, R. Wu, M. Xing, H. Shen, L.S. Li, X. Chen, Robust synthesis of bright multiple quantum dot-embedded nanobeads and its application to quantitative immunoassay, Chem. Eng. J. 361 (2019) 499–507.

[20] Z. Popovic, W. Liu, V.P. Chauhan, J. Lee, C. Wong, A.B. Greytak, N. Insin, D. G. Nocera, D. Fukumura, R.K. Jain, M.G. Bawendi, A nanoparticle size series for in vivo fluorescence imaging, Angew Chem. Int. Ed. Engl. 49 (46) (2010) 8649–8652.

[21] H. Xie, E. Chen, Y. Ye, S. Xu, T. Guo, Highly stabilized gradient alloy quantum dots and silica hybrid nanospheres by core double shells for photoluminescence devices, J. Phys. Chem. Lett. 11 (4) (2020) 1428–1434.

[22] Y. Zhao, C. Zhou, R. Wu, L. Li, H. Shen, L.S. Li, Preparation of multi-shell structured fluorescent composite nanoparticles for ultrasensitive human procalcitonin detection, RSC Adv. 5 (8) (2015) 5988–5995.

[23] L. Huang, T. Liao, J. Wang, L. Ao, W. Su, J. Hu, Brilliant pitaya-type silica colloids with central-radial and high-density quantum dots incorporation for ultrasensitive fluorescence immunoassays, Adv. Funct. Mater. 28 (4) (2018) 1–11.

[24] J. Zhou, M. Ren, W. Wang, L. Huang, Z. Lu, Z. Song, M.F. Foda, L. Zhao, H. Han, Pomegranate-inspired silica nanotags enable sensitive dual-modal detection of rabies virus nucleoprotein, Anal. Chem. 92 (13) (2020) 8802–8809.

[25] C. Yuan, Y.T. Deng, X.M. Li, C.F. Li, Z.D. Xiao, Z. Liu, Synthesis of monodisperse plasmonic magnetic microbeads and their application in ultrasensitive detection of biomolecules, Anal. Chem. 90 (13) (2018) 8178–8187.

[26] J. Aldana, Y.A. Wang, X.G. Peng, Photochemical instability of CdSe nanocrystals coated by hydrophilic thiols, J. Am. Chem. Soc. 123 (36) (2001) 8844–8850.

[27] Y. Katayama, T. Ohgi, Y. Mitoma, E. Hifumi, N. Egashira, Detection of influenza virus by a biosensor based on the method combining electrochemiluminescence on binary SAMs modified Au electrode with an immunoliposome encapsulating Ru (II) complex, Anal. Bioanal. Chem. 408 (22) (2016) 5963–5971.

[28] D. Li, J. Wang, R. Wang, Y. Li, D. Abi-Ghanem, L. Berghman, B. Hargis, H. Lu, A nanobeads amplified QCM immunosensor for the detection of avian influenza virus H5N1, Biosens. Bioelectron. 26 (10) (2011) 4146–4154.

[29] H. Bai, R. Wang, B. Hargis, H. Lu, Y. Li, A SPR aptasensor for detection of avian influenza virus H5N1, Sensors 12 (9) (2012) 12506–13518.

[30] D. Guo, M. Zhuo, X. Zhang, C. Xu, J. Jiang, F. Gao, Q. Wan, Q. Li, T. Wang, Indium-tin-oxide thin film transistor biosensors for label-free detection of avian influenza virus H5N1, Anal. Chim. Acta 773 (2013) 83–88.

[31] Y. Wang, Q. Ruan, Z.C. Lei, S.C. Lin, Z. Zhu, L. Zhou, C. Yang, Highly sensitive and automated surface enhanced Raman scattering-based immunoassay for H5N1 detection with digital microfluidics, Anal. Chem. 90 (8) (2018) 5224–5231.

[32] A. Petherick, Developing antibody tests for SARS-CoV-2, Lancet 395 (2020) 1101–1102, 10230.